Available at www.sciencedirect.com

ScienceDirect

journal homepage: www.elsevier.com/locate/he

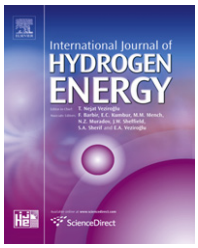

Technical Communication

Hydrogen fuel cell hybrid scooter (HFCHS) with plug-in features on Birmingham campus

*Jin Lei Shang, Bruno G. Pollet**

PEM Fuel Cell Research Group, Centre for Hydrogen and Fuel Cell Research, The University of Birmingham, Edgbaston Road, Birmingham B15 2TT, UK

ARTICLE INFO

Article history:
Received 24 June 2010
Received in revised form
4 August 2010
Accepted 18 August 2010
Available online 26 September 2010

Keywords:
Electric vehicle (EV)
Hydrogen fuel cell vehicle (HFCHV)
Plug-in hybrid ev (PHEV)
Battery electric vehicle (BEV)

ABSTRACT

A commercially available 'pure' lead-acid battery electric scooter (GoPed) was converted to a hydrogen fuel cell battery hybrid scooter (HFCHS) in views of investigating the effect of hybridisation on driving duty cycles, range, performance, recharging times, well-to-wheel CO_2 footprint and overall running costs. The HFCHS with plug-in features consisted mainly of a 500 W hydrogen PEM Fuel Cell stack connected to four 12 V 9 Ah lead-acid batteries and two hydrogen metal-hydride canisters supplying pure hydrogen (99.999%) and also acting as heat sink (due to endothermic hydrogen desorption process). In this study, the HFCHS urban driving cycle was compared with that of a conventional petrol and 'pure' battery electric scooter. The energy consumed by the HFCHS was 0.11 kWh/km, with an associated running cost of £0.01/km, a well-to-wheel CO_2 of 9.37 g CO_2/km and a maximum range of 15 miles. It was shown that the HFCHS gave better energy efficiencies and speeds compared to battery and petrol powered GoPed scooters alone.

1. Introduction

The concentration of greenhouse gases (GHG) in the earth's atmosphere is steadily increasing and creating changes in the world's climate. Recent studies showed that nearly a third of GHG emissions in the world [1] originate from the combustion of fossil fuels in internal combustion engine (ICE) vehicles. In Europe, the European Commission aims at reducing CO_2 emissions from new vehicles to an average of 130 g/km by the year 2012 and of 125 g/km by 2015 [2] with a longer term target of 100 g/km by 2020.

In many Asian and South American cities, petrol powered scooters are popular means of transport due to limited space caused by large population density in cities [3]. In these areas of the world, scooters are a more affordable option than automobiles [4]. However, the infrastructure in urban cities does not support an extensive transport network as well as parking spaces. Scooters are therefore more popular as they can be manoeuvred around traffic more easily than larger vehicles, especially in congested roads and take less parking space. Scooters are different from cars as they are not normally equipped with advanced engine management and catalytic converter systems to reduce harmful emissions. It was shown by Sripakagorn and Limwuthigraijirat [5] that conventional petrol motorcycles emit 95% more pollutants than larger sport utility vehicles due to the lack of installed emission control technologies.

Recently, Zero Emission Vehicles (ZEVs) have received a lot of attention worldwide. For example, battery electric vehicles (BEVs) and hydrogen fuel cell vehicles (HFCVs) are seen to be

* *Corresponding author*. Tel.: +44 (0)7554116546; fax: + 44 (0)121 414 5377.
E-mail address: b.g.pollet@bham.ac.uk (B.G. Pollet).
URL: http://www.polletresearch.com

0360-3199/$ – see front matter © 2010 Professor T. Nejat Veziroglu. Published by Elsevier Ltd. All rights reserved.
doi:10.1016/j.ijhydene.2010.08.075

Table 1 – Parameters for mathematical model.

	Parameters
$m = 57$	Vehicle mass (kg)
$m_G = 137$	Mass including driver (kg)
$P_{Tot} = 0.8$	Total power available (kW)
$\eta = 80\%$	Vehicle transmission efficiency
$P_{Wheels} = 0.704$	Power delivered to the wheels (kW)
$C_D = 1.3$	Drag coefficient
$A_f = 0.6$	Frontal area (m^2)
$C_D \times A_f = 0.718$	m^2
$h = 0.2$	Height of the centre of gravity (m)
$L = 1.2$	Wheelbase length (m)
$WD_f = 20\%$	Weight distribution (front)
$f_0 = 0.015$	Rolling resistance coefficient
$f_1 = 6.25 \times 10^{-5}$	Rolling resistance coefficient
$\rho = 1.2$	Air density (kg/m^3)
$g = 9.81$	Gravity (m/s^2)

a possible solution to tackling GHG emission. Major global automotive manufacturers such as Honda (FCX Clarity), Nissan (FCV X-trail) and Daimler-Chrysler have invested significant amounts on R&D for fuel cell vehicles. Some prototypes using a PEMFC stack up to 100 kW at a cost of $300,000 have ended up having a total vehicle cost of up to $2 million. However, recently Toyota has announced a price tag of $50,000 for its first hydrogen fuel cell vehicle [6]. Nevertheless, there are three main problems associated with fuel cell vehicles: (i) there are insufficient demonstration vehicles in the field to give adequate statistics on performance and cost in 'real-world' situations; (ii) vehicles are custom made and too costly for the consumer who typically only wishes to spend around £15,000 for a 'green' vehicle; and (iii) difficulty meeting existing legislation.

Another major obstacle to the widespread deployment of fuel cell vehicles is the availability of component materials. On the other hand, BEVs may offer an interim solution, but the limited range (up to 100 miles on full charge) and long recharge times (up to 8 h) properties does not fulfil the customers' demand and expectations leading to 'range anxiety'. However, HFCHVs with integrated plug-in systems may provide a cost-effective [7] alternative to solely HFCVs and traditional plug-in BEVs. Therefore, bridging the gap between today's BEVs and future's fuel cell vehicles is possible. It has also been demonstrated that fuel cell systems can operate under steady state and dynamic conditions with a tank-to-wheel efficiency of ca. 30% in specific driving cycles [8–11].

In this communication, we report a study of a hydrogen fuel cell battery electric vehicle (scooter) running on a 500 W hydrogen PEM Fuel Cell stack (used as range extender) with four 12 VDC lead-acid batteries.

2. Experimental

The scooter used for these experiments was a 2008 battery electric GoPed ESR750H [12]. The original scooter had four

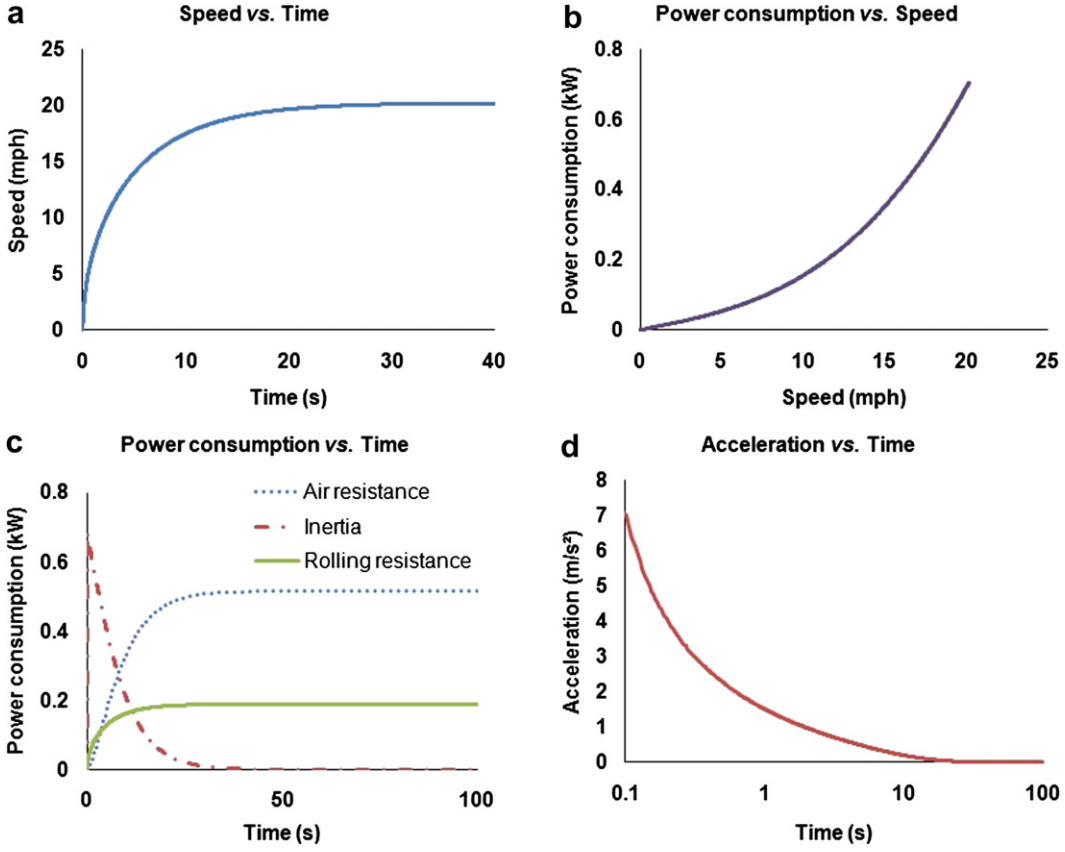

Fig. 1 – Mathematical Performance of modelling – (a) speed *vs.* time; (b) power consumption *vs.* speed; (c) power consumption *vs.* time; (d) acceleration *vs.* time.

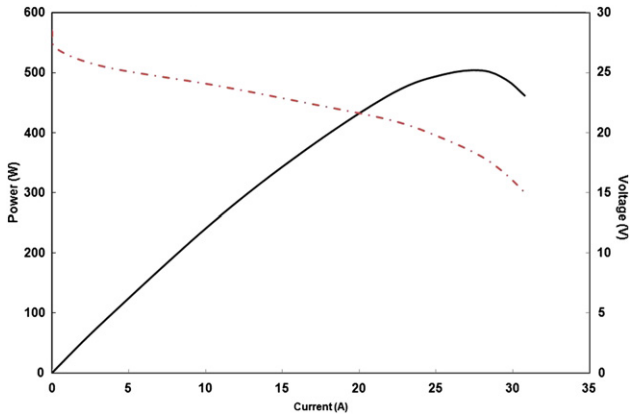

Fig. 2 – Horizon Fuel Cell 500 W PEMFC stack characteristics showing cell voltage (dotted line) and power (solid line) *vs.* current.

lead-acid batteries powering a 24 V brushed DC electric motor with "Electro Head" finned heat sink capable of producing over 1HP in continuous operation and reaching a top speed of 20 mph. The manufacturer claims that the maximum riding range is 8 miles in ideal conditions (flat ground and no stops) [12]. The modification of the scooter – HFCHS – was designed for driving on the University of Birmingham campus consisting of flat, up hills and down hills areas.

2.1. *Modelling and theory*

In order to obtain the power required and foresee the performance of the hybridisation, a mathematical model was developed (Appendix 1) using specific parameters shown in Table 1. Fig. 1 clearly shows that a top speed of 20 mph can be easily achieved with a good acceleration at a required overall power of 650 W. In our conditions, a 500 W PEMFC stack was used for the hybridisation.

2.2. *Components*

2.2.1. *PEMFC stack*

A 500 W air cooled PEMFC (Horizon Fuel Cells) of a maximum efficiency of 40% at 21 VDC and a maximum current output of 24 A was used (Fig. 2). This stack consisted of 36 cells with a rated hydrogen consumption of 6.5 NL/min. It had an external 12 V battery power source to supply the hydrogen inlet valve, the hydrogen purging valve and the cooling fans [13].

2.2.2. *Hydrogen storage*

Two Highland 300 hydrogen metal-hydride canisters were used (dimensions of 50 × 105 × 420 mm and weight of 6.5 kg), storing 600 NL of pure hydrogen (99.999%) with a discharge pressure of 0.3 bar and a flow rate of 2–3 NL/min at ambient (20 °C). The two metal-hydride storage canisters could take up 54 g of hydrogen equivalent to 1.8 kWh of energy. The metal-hydride storages were connected to the PEMFC stack via a pressure regulating valve to control the pressure output. The cylinders were attached on the top of the motor in order to use the motor heat to boost the hydrogen release, as well as to cool down the motor temperature. The charging time was less than 20 min in an ice-cold water bath.

2.2.3. *Battery*

Four 12 VDC 12 Ah valve regulated sealed lead-acid rechargeable batteries were fitted under the scooter board. Two batteries were connected in series and then paralleled with two others. These batteries had a total power of 576 Wh, capable of discharging a maximum current of 360 A in 5 s [14]. The batteries also continuously supplied 15 W of power to the PEMFC stack controller through a 24–1 2V DC–DC converter.

2.2.4. *Motor*

The 24 V DC brush type motor with aluminum heat sink of 80% efficiency was capable of producing 800 W of power in continuous operation and up to 2500 W in short period of times.

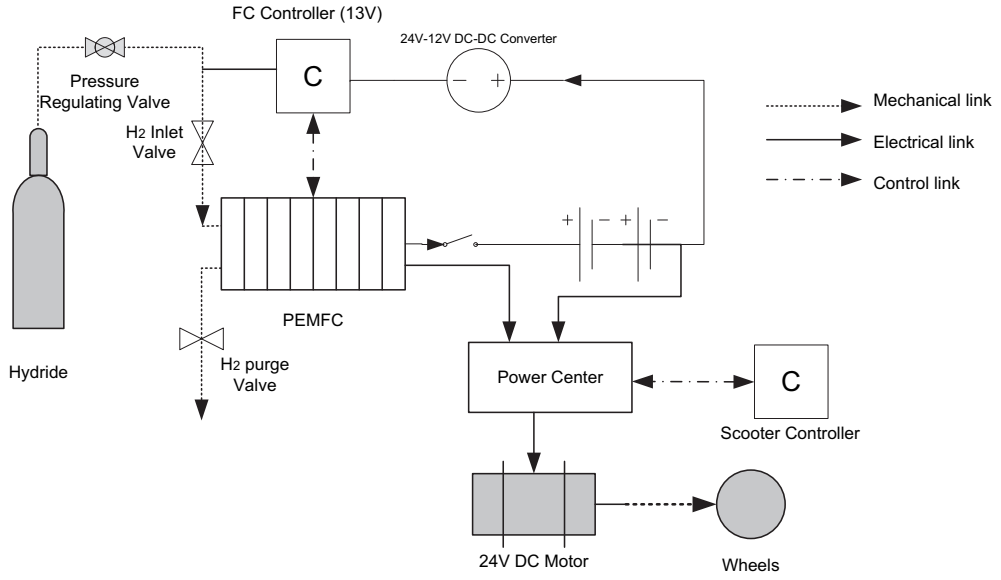

Fig. 3 – Component diagram of the HFCHS showing all components and electrical drive system layout.

2.3. Data collection

In order to determine the range and performance of the HFCHS under different driving conditions, data logging was performed. The speed, power and range of the HFCHS were logged for each experiment. The current was monitored using a current clamp adaptor (TECPEL CA1000D) connected to a data logger (Grant Squirrel 2010). The power output of the PEMFC stack was also logged.

A GPS logging system (Racedrive 2090) was installed on board of the HFCHS to monitor speed and distance completed. The GPS results combined with the power data allowed clear indication on how the power train performed. Fig. 3 shows the system integration of components and Fig. 4 shows the HFCHS.

3. Results and discussion

Fig. 5 shows the performance of the HFCHS when driving at low battery level (SOC = 20%). The green plot shows the speed of the HFCHS with time where an average speed of 8–10 mph is achieved. The motor current was between 20 A and 30 A (blue plot) giving a motor power demand of 480 W–720 W. The pink plot represents the current output from the PEMFC stack, starting from 12 A and gradually increasing up to 18 A, giving a power output of 250–380 W. The figure also shows that the power demand from the motor is higher than the power output from the PEMFC stack, and the extra power required comes from the batteries. For this experiment, the run lasted for 42 min before the PEMFC stack cut off due to the lack of hydrogen in the cylinders.

Fig. 6 shows the performance of the HFCHS when driving at full battery level (SOC = 100%). Here, the batteries were fully charged in 5 h. In our conditions, the average speed was around 8 mph with again, a motor power demand of 480–720 W. Unlike our previous tests at low battery level, the

Fig. 4 – Picture of the HFCHS.

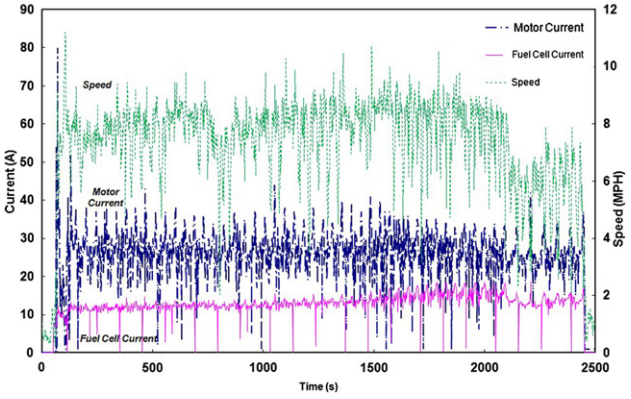

Fig. 5 – Performance of HFCHS when the batteries are low [SOC = 20%]. Speed *vs.* time (green plot); Motor current *vs.* time (blue plot); fuel cell current *vs.* time (pink plot). (For interpretation of the references to colour in this figure legend, the reader is referred to the web version of this article).

PEMFC stack power output varied between 200 W and 320 W, in other words less power was required from the stack at full battery SOC. This test lasted longer, i.e. over 1 h. Obviously, during these experiments, the PEMFC stack functioned below its rated maximum power, possibly due to the following reasons: a) the metal-hydride canisters cannot supply enough hydrogen to the stack, b) the power demand is low or/and c) lack of power management system. This is further explained below.

3.1. Hydrogen supply

The metal-hydride canisters were 'charged up' directly from high purity hydrogen (99.999%) at a pressure of 15 bar. It only took 20 min for full charge at room temperature but only 12 min at 0 °C (ice–water bath) at 25 bar. The PEMFC stack consumes 6.5 NL/min to reach a maximum power of 500 W,

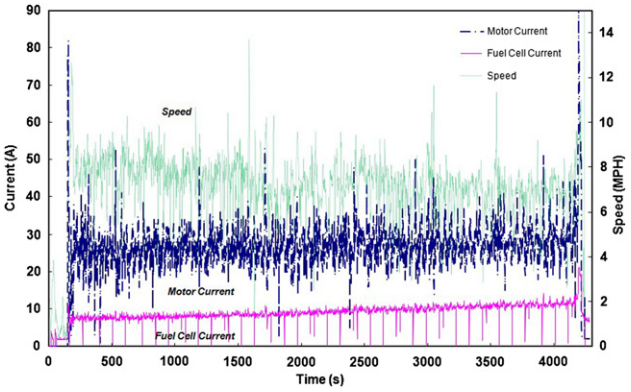

Fig. 6 – Performance of HFCHS when the batteries are fully charged [SOC = 100%]. Speed *vs.* time (green plot); Motor current *vs.* time (blue plot); fuel cell current *vs.* time (pink plot). (For interpretation of the references to colour in this figure legend, the reader is referred to the web version of this article).

Table 2 – Charactersitics and comparison of the electric, petrol and hybrid scooter.

	GoPed FC Plug-in	GoPed Plug-in	GoPed (29cc)
Vehicle Cost	£3000	£1200	£800
MPG Equivalent	500mpg (H_2)	383mpg	100mpg
Energy Efficiency	37–75%	75%	20%
Tail-Pipe Emission	None/H_2O	None	Harmful Air Pollutions
Well-to-Wheel CO_2	9.37–40.95 g CO_2/km	24.07 g CO_2/km	90–120 g CO_2/km
Running Cost on Fuel	£0.01–£0.11/mile	£0.01/mile	£0.06/mile
Refuelling Time	15 min – 5 h	5 h	1 min
Range	15 miles	8 miles	32 miles
Top Speed	25.8 mph	20 mph	24 mph
Noise Level	55 db	55 db	75 db

however, in our conditions; the metal-hydride canisters only supplied 2–3 NL/min of hydrogen at room temperature. Although the metal-hydride canisters were placed onto the 'hot' motor to gain some heat, this design did not seem to work to achieve a minimum flow rate of 6.5 NL/min to the stack; for example, the metal-hydride canisters surface temperature dropped from 30 °C to 0 °C in 20 min, and at this point, the flow rate dropped even further. Furthermore, it was observed that the hydrogen was wasted during fuel cell purging cycles, i.e. with time duration of 1 s at a flow rate of 2–3 NL/min at interval times of 10 s between each purging. We found that during the purging process, ca. 1/10th of the hydrogen energy was wasted.

3.2. *Power management*

As seen from Figs. 5 and 6, the PEMFC stack always functioned below its optimum power due to the lack of advanced power management systems. For example, the motor withdraws power from the highest voltage power source first, in this case the lead-acid batteries at 22 V (Fig. 2), compared with 18 V for the PEMFC stack. In our conditions, by using a DC–DC converter, the load is higher than the fuel cell rated power and the batteries work in order to provide the power needed to satisfy the load.

Even with the lack of power management systems, the range of the HFCHS was 15 miles after 70 min riding at a top speed of 25.8 MPH. For comparison purposes, experiments on 'pure' battery and petrol scooters were performed as shown in Table 2. The table shows that HFCHS offers many advantages over electric and petrol scooters, for example, higher energy efficiency (up to 75%), lower running costs, higher speed and better MPG equivalent. For example, using two 600 NL (0.054 kg) hydrogen metal-hydride canisters give an energy of 1.8 kWh or 6.48×10^6 J and a 40% efficient PEMFC stack gives at total energy of 0.72 kWh which is higher than battery only powered and lower than petrol powered scooters of 0.42 kWh and 1.71 kWh respectively. However, the estimated cost of the HFCHS is much higher than that of the pure electric and petrol scooters. For example, the donor vehicle GoPed costs around £1200 (inc. seat and basket kit), the 500 W PEMFC stack costs ca. £1200, the Highland metal-hydrides cost approximately £500, and other components like DC–DC converters, switches cost approximately £50. The total cost of this HFCHS is ca. £3000 compared with only £800 for the pure electric GoPed. Furthermore, well-to-wheel CO_2 footprint values showed that the HFCHS gives a total of 9.37 g CO_2/km to 40.95 g CO_2/km depending on where the hydrogen comes from (Table 3). For comparison purposes, the scooter only powered by batteries gives a well-to-wheel CO_2 footprint of 24.07 g CO_2/km, which could be lowered if the produced electricity originates from renewable sources. Appendix 2 shows detailed well-to-wheel CO_2 emission calculations to ascertain the environmental impact of the scooter when 'hybridised' compared to battery alone.

4. Conclusions

In this study, we showed that the hybridised scooter offers many advantages over petrol and battery powered scooters such as acceptable ranges, higher speeds, better MPG equivalent, higher energy efficiencies and lower well-to-wheel CO_2 footprint. With the plug-in feature, the HFCHS benefits from a smaller fuel cell stack running at a higher efficiency, in turns extending the life of the fuel cell and the battery pack

Table 3 – Well-to-wheel carbon footprint from different energy sources.

H_2 Source	g CO_2/kg H_2	H_2 Consumed/g	Total CO_2 produced/g	Range/km	Total Carbon Emission g CO_2/km
Steam Methane Reforming (SMR)	11374.90	0.054	614.20	15	40.95
Solar	3804.00	0.054	205.42	15	13.69
Wind	2604.00	0.054	140.62	15	9.37
Hydro	3324.00	0.054	179.50	15	11.97
Biomass	4284.00	0.054	231.34	15	15.42

life and lowering the overall costs when running on battery only. However, the HFCHS was not optimized and further work is required, for example, a) acceptable supplies of hydrogen to the stack in order for the PEMFC to work at its rated power of 500 W and b) the installation of a power management system.

Acknowledgement

The authors would like to thank Advantage West Midlands (AWM) under the Birmingham Science City Initiative and EPSRC (Contract No: EP/E034888/1).

Appendix 1.

There are four forces opposing the motion of a vehicle, namely: the rolling friction force (F_r), the air resistance force (F_a), the inertia force (F_i) and the gravitational force (F_g) as shown below [15]:

$$F_r = mg\mu_r \quad (1)$$

$$F_a = \frac{\rho}{2} C_D A_f v^2 \quad (2)$$

$$F_i = m\dot{v} \quad (3)$$

$$F_g = mg\ \sin(\theta) \quad (4)$$

where m is the vehicle mass (kg), ρ is the air density (kg/m^3) along the longitudinal axis, C_D is the aerodynamic resistance coefficient or drag coefficient, A_f is the vehicle frontal area (m^2), v is the vehicle velocity (m/s), $\dot{v}$ is the vehicle acceleration, θ is the grade angle, g is the gravitational acceleration (9.81 m/s^2) and μ_r is the rolling resistance coefficient.

To estimate the average power required for the scooter, we assumed a grade angle of zero and neglected the inertia force (F_i). A typical μ_r value for properly inflated scooter tyres on hard pavement is 0.015. The scooter with auxiliary has a mass of 57 kg and assuming a rider mass of 80 kg, the resisting force of rolling friction (F_r) on a level road can be calculated as shown below:

$$F_r = mg\mu_r = [(80 + 57) \times 9.81] \times (0.015) = 20.16N \quad (5)$$

NB1: This force is nearly independent from the vehicle speed.

The air resistance force (F_a) was calculated by using the following parameters: the drag coefficient (C_D) which depends on the shape and the silhouette area of the vehicle (A_f) (seen from the front), the air density ($\rho \approx 1.2$ kg/m^3 at sea level and STP) and the scooter speed (v). Values of C_D for a typical scooter range from 0.60 to 1.3; in our conditions, the GoPed is not aerodynamic and $C_D = 1.3$ and $A_f = 0.6$ C_D values were used. Assuming that the maximum speed of this scooter is 20 mph (i.e. 8.94 m/s), the air resistance force (F_a) can be determined using Equation (6):

$$F_a = \frac{\rho}{2} C_D A_f v^2 = \frac{1.2}{2} \times (1.3) \times (0.6) \times (8.94)^2 = 37.41N \quad (6)$$

Therefore in ideal conditions (no inertia and at flat ground levels), the total power required to overcome the total friction force ($F_r + F_a$) is:

$$P = (Fr + Fa)v = (20.16 + 37.41) \times (8.94) = 514.68\ \text{W} \quad (7)$$

Hence the average power required for this scooter is around 500 W.

To estimate the performance of the scooter, a simulation (using MS Excel) was performed by assuming that:

(i) the scooter started at a rest time, $t = 0$ s and accelerated at full power until time, $t = 100$ s.
(ii) the grade angle (θ) is zero and hence $F_g = 0$ with the inertia force (F_i) now being considered.

NB2: Other parameters used in the simulation are show in Table 1.

In our simulation, the power required to overcome air resistance (P_a) and rolling resistance (P_r) were calculated using Equations (8) and (9) respectively:

$$P_a = \frac{\rho}{2} C_D A_f v^3 \quad (8)$$

$$P_r = mg\mu_r v \quad (9)$$

The remaining power (i.e. the total motor output minus the sum of P_a and P_r) was assumed to overcome inertia resistance (P_i). The vehicle acceleration was calculated from this power, and was limited by the adhesion of the tyres to the ground. The force used to overcome the air resistance force (F_a), the rolling resistance force (F_r) and the inertia resistance force (F_i) were calculated Equations (1)–(3) and are shown in Fig. 1.

Appendix 2.

A well-to-wheel CO_2 emission calculation was performed to ascertain the environmental impact of the scooter when hybridised compared to battery only.

The CO_2 burden of electricity when charging the scooter was calculated from reference [16]. The total CO_2 production from electricity generation was used, as well as the global power production, to give a value in g CO_2/kWh. Global values were taken into account as there are large variations between countries depending on the level of carbon reduction technologies and legislation implemented (Table I).

Table A1 – CO_2 burden from electricity generation.

Power/kWh	g CO_2/kWh	g CO_2	Battery Range/km	g CO_2/km
0.576	535.07	308.2	12.8	24.07

For the hydrogen production, two different routes were considered, hydrogen production using renewable energy and hydrogen production from steam reforming of natural gas (mainly methane - SMR). Table II shows the CO_2 produced for several different renewable energy sources as well as for steam reforming of natural gas.

Table A2 – CO_2 burden from various Hydrogen production routes [17].

Method	g CO_2/kg H_2 [g/kg]	kg CO_2 eq. [kg/MJ]
SMR	10,662.1	0.085
Solar	2160	0.018
Wind	960	0.008
Hydro	1680	0.014
Biomass	2640	0.022

Once hydrogen has been produced, there is a further energy input to compress the gas to either a liquefied or compressed gas state so that it can be easily transported. Compression values are given for hydrogen produced by the SMR and the renewable routes as shown in Table III.

Table A3 – CO_2 burden for compressing H_2 [18].

Source	g CO_2/kg H_2 [g/kg]
Renewable sources	1644
Natural Gas	712.8

REFERENCES

[1] Silva C, Ross M, Farias T. Evaluation of energy consumption, emissions and cost of plug-in hybrid vehicles. Energy Convers Manag 2009;50(7):1635–43.

[2] Gonder JSA. Measuring and reporting fuel Economy of plug-in hybrid electric vehicles. World Electric Vehicle Assoc 2007;1.

[3] Tso C, Chang S-Y. A viable niche market – fuel cell scooters in Taiwan. Int J Hydrogen Energy 2003;28(7):757–62.

[4] Colella WG. Market prospects, design features and performance of a fuel cell-powered scooter. J Power Sources 2000;86(1–2):255–60.

[5] Sripakagorn A, Limwuthigraijirat N. Experimental assessment of fuel Cell/supercapacitor hybrid system for scooters. Int J Hydrogen Energy 2009;34(15):6036–44.

[6] visited on, www.fuelcellstoday.com; 4th June 2010.

[7] Kendall K, Pollet BG, Dhir A, Staffell I, Millington B, Jostins J. Hydrogen Fuel cell hybrid vehicles for Birmingham campus, J. Power Sources, doi:10.1016/j.jpowsour.2009.12.012.

[8] Corbo P, Migliardini F, Veneri O. Performance investigation of 2.4 kW PEM fuel cell stack in vehicles. Int J Hydrogen Energy 2007;32(17):4340–9.

[9] Corbo P, Corcione FE, Migliardini F, Veneri O. Energy management in fuel cell power trains. Energy Conversion Manage 2006;47(18–19):3255–71.

[10] Corbo P, Corcione FE, Migliardini F, Veneri O. Experimental study of a fuel cell power train for road transport application. J Power Sources 2005;145(2):610–9. 18.

[11] Philipps F, Simons G, Schiefer K. Dynamic investigation of PEFC stacks in interaction with the air supply system. J Power Sources 2006;154(2):412–9.

[12] Werks PM. ESR750Hover, from, http://www.goped.com/Products/ESR750Hover/Default.asp (2004).

[13] Horizon 500 W Proton exchange membrane fuel cell user manual; 2009.

[14] B.B. Valve regulated lead acid battery manual; 2008, 8.

[15] Gillespie TD. Fundamental of vehicle dynamics. Society of Automotive Engineers; 1992.

[16] Malla S. CO_2 emissions from electricity generation in Seven Asia-Pacific and North American countries: a decomposition analysis. Energy Policy 2009;37(1):1–9.

[17] Koroneo C, Dompros A, Roumbas G, Moussiopoulos N. Life cycle assessment of hydrogen fuel production processes. Int J Hydrogen Energy 2004;29(14):1443–50.

[18] Granovskii M, Dincer I, Rosen MA. Life cycle Assessment of hydrogen fuel cell and Gasoline vehicles. Int J Hydrogen Energy 2006;31(3):337–52.